Eric Haentzsche, Moritz Frauendorf, Andreas Nocke, Chokri Cherif, Michaela Reichardt, Marko Butler, Viktor Mechtcherine

Multifunctional components from carbon concrete composite C³ – integrated, textile-based sensor solutions for in situ structural monitoring of adaptive building envelopes

Erstveröffentlichung in / First published in:

Textile Research Journal. 2018, 88(23), S. 2699 – 2711 *[Zugriff am: 07.08.2019]*. SAGE journals. ISSN 1746-7748.

DOI: https://doi.org/10.1177/0040517517729385

Textile Research Journal

Original article

Textile Research Journal
2018, Vol. 88(23) 2699–2711

DOI: 10.1177/0040517517729385
journals.sagepub.com/home/trj
SAGE

Multifunctional components from carbon concrete composite C³ – integrated, textile-based sensor solutions for in situ structural monitoring of adaptive building envelopes

Eric Haentzsche[1], Moritz Frauendorf[1], Andreas Nocke[1], Chokri Cherif[1], Michaela Reichardt[2], Marko Butler[2] and Viktor Mechtcherine[2]

Abstract

This contribution will introduce carbon-reinforced concrete components (so-called carbon concrete composites, or C³) with sensor functionalities for innovative building envelopes. For a continuous in situ structural monitoring, these textile-reinforced concrete components are equipped with textile sensor networks consisting of resistive carbon fiber sensors (CFSs), which are integrated into the carbon fiber non-crimp fabrics of the concrete reinforcement by multiaxial warp-knitting. The in situ CFSs, consisting of 1 k or 50 k carbon fiber roving with added staple fiber/multifilament dielectric cladding, are later integral to the load-distributing elements of the concrete component, and elongations within these are easy to record with good correlation to ohmic resistance changes. Gage factors of $k = 0.52–1.23$ at linearity deviations of $A_{Lin} = 4.0–8.7\%$ are feasible. This allows a monitoring of C³ building envelopes for structural mechanical changes caused by physical changes within the component through mechanical or thermal loads or deformation and cracks.

Keywords

c³ carbon concrete composite, carbon fiber, resistive fiber strain sensor, in situ sensor systems, load monitoring

Introduction

TU Dresden and the Rheinisch-Westfaelische Hochschule Aachen have been involved in research projects regarding continuous fiber-reinforced concrete since 1992 within the scope of the Collaborative Research Center SFB 528[1] and SFB 532.[2] This material is an innovative type of concrete composite material, whose reinforcement structure consists of warp-knitted fabrics made from non-corrosive, alkali-resistant glass or carbon fiber (CF) bearing the load distribution. C³ carbon concrete composite is particularly important, as CF requires only 5.0 mm of concrete cover thickness to be corrosion-resistant, instead of the 15–50 mm prescribed for steel by standards EN 1992-1-1 (EC 2) and DIN 1045-1. This significantly reduces wall thickness and weight. In contrast to conventional steel reinforcements $R_{M,St} < 0.64$ GPa, the higher tensile strength $R_{M,CF} = 4.0$ GPa in combination with the CF density ($\rho_{CF} = 1.77$ g/cm³) reduced by 77% allows for much lighter concrete reinforcement structures and a further reduction of the total weight. The TUDALIT® (DIBt general technical approval N° Z-31.10-182) reinforcement structure from CF roving[3] for the production of lightweight C³ components

[1]Institute of Textile Machinery and High Performance Material Technology (ITM) at Technische Universitaet Dresden, Germany
[2]Institute of Construction Materials (IFB) at Technische Universitaet Dresden, Germany

Corresponding author:
Eric Haentzsche, Institute of Textile Machinery and High Performance Material Technology (ITM) at Technische Universitaet Dresden, Hohe Strasse 6, 01069 Dresden, Saxony, Germany.
Email: eric.haentzsche@tu-dresden.de

(Figure 1) consists of an open, biaxially reinforced, grid-like non-crimp fabric (NCF) in a 0°/90° arrangement.

According to the TUDALIT® specifications (Deutsches Institut für Bautechnik DIBt – General technical approval N° Z-31.10-182 (30.11.2016): Method for the strengthening of ferroconcrete by TUDALIT – Textile reinforced concrete), the reinforcement thread system running in the major load direction (0°) of the projected C^3 component consists of CF rovings (3.3 ktex and 50,000 individual filaments, i.e. 50 k). The CF roving in the 90° direction has only 12,000 individual filaments and a titer of 0.8 ktex because transversal contractions under purely tensile strain can be absorbed by the compressive strength $R_D = 0.05$–0.09 GPa of the surrounding concrete. No further reinforcement is necessary normal to the major load direction. The thread CF systems of the NCF, which are placed orthogonally to each other, have a grid opening size of 10.7 mm × 14.3 mm (Figure 2). They are fixed to be force-fit and displacement-proof by means of additional polyester (PES) binder yarns (cf. Figure 2(a), red yarns). The NCF is produced on a multiaxial warp-knitting machine with a maximum working width of 2.54 m.

As constructions and carrier structures from reinforced concrete are designed to last longer than 25 years, optical assessments of the structure can only be conducted externally and at longer intervals, which does not allow a secure estimate of the residual carrying capacity. Therefore, measuring methods and equipment designed to continuously report on mechanical strains and provide event-oriented information on structural shifts within the component are in high demand. Suitable sensors must be compatible with composites, robust enough to resist physical and chemical influences during concrete pouring and reliable in the short and long term. The scalable sensors should also be inserted into the textile reinforcement structure in order to save costs. Any necessary additional work is limited to electrical contacting or coupling to measuring devices outside the C^3 components. Apart from established measuring possibilities like superficial strain gages and fiber-optical sensors[4,5] or imaging methods like

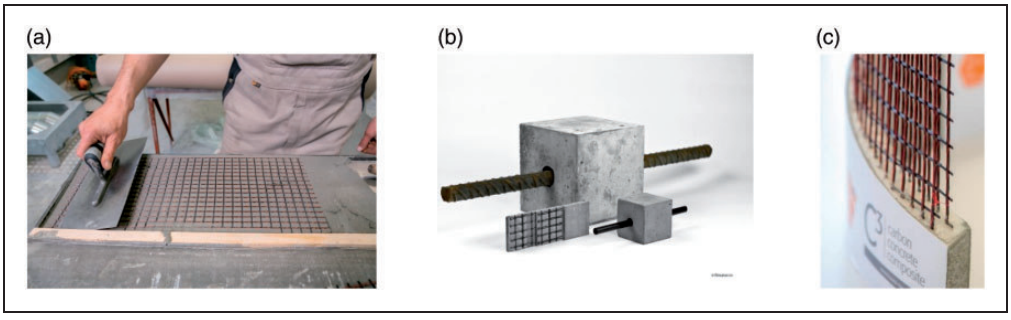

Figure 1. From textile structure to carbon concrete composite C^3 (a; © Joerg Singer); resource-conserving thin-walled C^3 components in comparison to ferroconcrete counterparts (b; © filmaton.tv); award-winning (German Sustainability Award 2015, Deutscher Zukunftspreis 2016) C^3 facade element of future buildings (c).

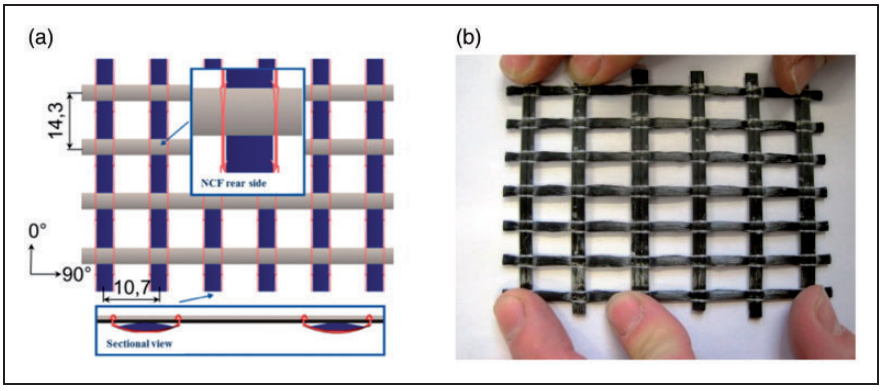

Figure 2. (a) Schematic structure (carbon fiber (CF) warp yarn: blue; CF weft yarn: grey; polyester binder yarn: red) and (b) real CF biaxial non-crimp fabric for the reinforcement of C^3 components (© Joerg Singer). (Color online only).

Acoustic Emission Analysis,[6] this article will only discuss fiber-based and textile-technologically integrated sensor concepts for straining measurement, as they enable real in situ load monitoring within the load bearing reinforcement structure of the C^3 component.

Recent research by Goldfeld et al.[7,8] demonstrated the general suitability of polyacrylonitrile-based CF rovings as integrally measured strain sensors in textile-reinforced concrete. The sensor-carrying reinforcement textile in this case consisted of a biaxial glass fiber (GF) NCF, in which individual GF warp threads were substituted with CF sensor threads. Additional measures for the cladding of the sensor yarn to prevent short circuits with the CF-NCF, which are usually taken in C^3 applications, were not required. Instead of the GF reinforcement fiber, the sensor thread was connected to the NCF in the warp direction (0°) by a pillar stitch construction. The determined gage factor $k \approx 1.0^7$ was significantly smaller than in conventional strain gages with gage factors in the range of $1.9 \leq k \leq 2.5$. This was due to the inhomogeneous strain field created along the integration and, thus, the active measuring length of the sensor yarn in the textile-reinforced concrete during crack formation. In other literature,[8] the k factors for such strain sensors were stated as $2.4 \leq k \leq 5.4$ for tensile and $-6.6 \leq k \leq -2.7$ for compression loads, without offering a detailed explanation. An interference of geometrical changes and the specific resistance (conductivity) of CF under mechanical strain was proposed as the reason for high sensitivity.

Wen et al.[9–11] described the use of electrical properties of mainly pitch-based CF in concrete structures for structural monitoring and strain measurement, with short CF being added to the concrete matrix up to the percolation threshold with the fiber volume content set at 0.2–1.0%. Resistance was determined by means of the four-probe method, where the geometrical and spatial arrangement of powering as well as current measuring contacts of the measuring device define the active measuring direction. This means that a volume-related change in resistance is measured instead of a length-related one, which would record longitudinal and transversal strain. The sensitivity in particular cases[12] was up to $k = 76$ at a strain equivalent of 1.5‰ and a fiber volume content of 0.8%. Wen et al.[11] used a 2 k CF roving instead of short CF as strain sensor, which was inserted into the concrete matrix as a layered unidirectional stack. The fiber volume content was set to a range of 2.6–7.2%. The determined sensitivity of such strain sensors was in the range of $16 \leq k \leq 57$ and thus 20–62 times higher than in comparable CF sensors contained in fiber-reinforced plastic or textile-reinforced composites of the type presented in this article. Partially irreversible changes in resistance due to strain-related degradation of the fiber–matrix interface were put forward as the cause. Yang and Wu[13] introduced another form of an integrated, CF-based strain sensor consisting of a stack of three layered CF rovings with 6 k, 6 k and 12 k filaments. This stack was glued onto pre-stressed concrete tendon with epoxy resin and then inserted into the concrete composite. The k factor achieved under cyclic strains up to 0.9‰ was $k = 330$. The production of such sensor types[13] cannot be implemented into the textile-technological production chain of the CF-NCF reinforcement structure. The sensor concept for C^3 is transferable insofar as the strength carrier (CF-NCF) can house the textile sensor component and both can be processed concomitantly into reinforcement structure fabrics.

Further research activity[14] presented meandering strain gages made from a 1 k CF roving (67 tex), applied to poly(vinyl acetate) (PVA)-based water-soluble nonwovens by means of Tailored Fiber Placement. After embroidering of the sensor, the PVA nonwoven was removed caustically, and the textile strain gage was simultaneously consolidated by means of an epoxy resin, which also insulated it electrically. The sensitivity of such CF strain gages inserted into a C^3 specimen (size $L \times W \times H = 400 \times 70 \times 10\,mm^3$) in the area of the neutral fiber was determined by four-point bending tests (maximum 0.5 mm bending) at $k = 1.7 \pm 7\%$. This parameter and the achieved sensitivity are comparatively high and comparable to conventional strain gages, although the CF strain gage was only attached via the concrete matrix, which was completely torn in the carrying state of steel and C^3 components. Despite the inhomogeneous strain field and the insertion in the area of the neutral fiber, the meandering strain sensor exhibited high sensitivity under bending loads.[14]

The use of textile reinforcement structures with intrinsic conductivity, for example, NCF made from CF roving with integrated insulated CF-based sensors, for in situ strain measuring and structural monitoring has rarely been discussed and will therefore be the focus of this contribution. The scientific and technical aspiration is for a secure cladding of CF roving used as a mechanical strain gage, which is then inserted into the textile reinforcement structure as a sensing and load-bearing part of the C^3 component. This is achieved using only noninvasive textile-technological fabric production processes.

Materials and methods

Resistive fiber sensors

Within this research project, two source materials from CF roving were used as integrable textile strain gages, each of which were fit with dielectric cladding by

different methods (cf. Table 1) and characterized in terms of their response characteristics in the C[3]. Type A CF roving with 67 tex was chosen for the CF integration into the NCF reinforcement structure because it represents the commercially available roving with the smallest yarn count. Therefore, it can be assumed that it has minimal influence on the mechanical behavior. Type B CF roving with 3300 tex was chosen for the substitution of the standard warp yarn system of the NCF reinforcement structure. It can act as both reinforcement and sensor thread.

For the measurement principle, the approach of strain measurement via piezo-resistive carbon fiber sensors (CFSs) was pursued. This was done by using the effect of strain-correlated resistance change (cf. Equations (1) and (2)) of the intrinsically electrically conductive CF, which was first identified by Owston in 1970.[15] The strain measurement of mechanical elongation transferred onto the CF is therefore indirectly determinable via the absolute change in resistance ΔR (cf. Figure 3(a)). Previous examinations made by the authors showed that CF is suitable as an in situ strain gage for the structural and strain monitoring of fiber-reinforced plastic components.[16–19]

For the purpose of comparison, the typical sensor characteristic values, which apply to strain gages (cf. Figure 3(b)), were used: the gage factor k (Equation (3)), the linearity deviation A_{Lin} (Equation (4)) from an assumed linear transfer characteristic curve and the hysteresis A_{Hys} (Equation (5)). The last two specific values represent the bias under equal cyclic loads

$$\Delta R = R - R_0 = \frac{U - U_0}{I_0} \tag{1}$$

Table 1. Physical values of electrically isolated carbon fiber sensor

Core material		Type A: 1 k CF roving	Type B: 50 k CF roving
Manufacturer		Toho Tenax Europe	SGL Carbon
Type		Tenax® HTA40 H15 1 k	Sigrafil® C30T050 EPY 50 k
Roving titer		67 tex	3300 tex
N° of filaments		1000	50,000
Filament diameter		7.0 µm	7.0 µm
Specific resistance		$1.6 \cdot 10^{-3}$ Ωcm	$1.5 \cdot 10^{-3}$ Ωcm
Original function in CF-NCF for C[3]		None; additive sensor thread	0° warp yarn thread
Cladding		Variant I DREF 4.0 ktex sliver of 60 mm PES staple fiber variant II BRAIDING 1.67 tex PES filament yarn	
Total titer	Variant I	356 ± 11 tex	4457 ± 48 tex
	Variant II	222 ± 2 tex	3723 ± 21 tex

CF: carbon fiber; NCF: non-crimp fabric.

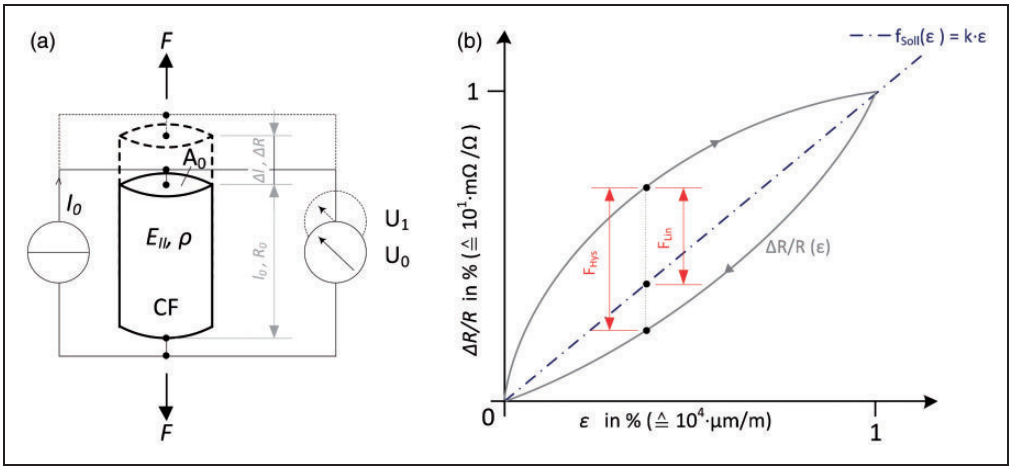

Figure 3. Measurement principle of carbon fiber (CF)-based textile strain gages (a) and method for the determination of specific sensor values (b).

$$\frac{\Delta R}{R_0} = f(\varepsilon) = \varepsilon\, k = \frac{\Delta l}{l_0} k \tag{2}$$

$$k = \frac{\Delta R/R_{0_{\max}} - \Delta R/R_{0_{\min}}}{\varepsilon_{\max} - \varepsilon_{\min}} \tag{3}$$

$$A_{Lin} = \frac{F_{Lin_{\max}}}{\Delta R/R_{0_{\max}} - \Delta R/R_{0\min}} = \frac{\max\left|\Delta R/R_0 - k\varepsilon\right|}{\Delta R/R_{0_{\max}} - \Delta R/R_{0_{\min}}} \tag{4}$$

$$A_{Hys} = \frac{F_{Hys_{\max}}}{\Delta R/R_{0_{\max}} - \Delta R/R_{0_{\min}}} \tag{5}$$

In Equations (1)–(5) the following formula symbols were used: $\Delta R/R_0$ means the relative change of CFS resistance as a ratio between its absolute resistance change ΔR and its basic resistance R_0; I_0 is the constant exciting current of the ohmmeter, U is the measured potential due to CFS tensile straining and U_0 the basic potential of the unstrained CFS; Δl is CFS elongation due to tensile straining; l_0 is CFS basic length (cf. Figure 3(b)).

To implement the CFS approaches, the application of dielectric cladding on the CFS was essential due to the conductivity of the CFs $\rho^{-1} = 0.15$–$0.17\,\mathrm{S{\cdot}m^{-1}}$, which were located near each other as sensors and reinforcement structure. This was necessary in order to record exclusively the strain along the integration path of the piezo-resistive CFS as a change in resistance resulting from load-induced geometry change. The influence of this piezo-resistive effect discovered originally by Bridgman[20] on the specific resistance is related to the load-induced change of resistance in CF by Wen and Chung[21] and others, but has not yet been separately quantified. Therefore, this article will not further examine phenomenological changes in conductivity caused by mechanical loads.

The cladding made from staple fiber and filament yarn PES were applied around the CF roving fed as the core yarn (Figure 4) either by friction-spinning (variant I) on a DREF-2000 friction spinning machine (Dr. Ernst Fehrer AG/Oerlikon[22]) or by braiding (variant II) on a braiding machine RU2/12-80 (August Herzog Maschinenfabrik GmbH & Co. KG). To produce the friction-spun yarns, the following parameters were set on the DREF-2000 spinning machine, depending on the CF roving fineness: 1500–4500 rpm spinning drum rotation, 4500 rpm opening roller rotation and 1300 kPa suction pressure, with which production speeds of up to 50 m/min were achieved. To produce the braided sensor variants, the CF roving was covered by six (for 1 k CF) or 12 (for 50 k CF) 16.7 tex PES filament threads at a production speed of 0.10 m/min. To determine the achieved ohmic leakage resistances of the differently cladded CFSs, a non-standardized, unique test setup was used, in which 0.5 m samples of each type were fixed between two copper plates. The sheet resistance between the copper electrodes, which did not touch otherwise, was then determined by means of a FLUKE 8846 precision ohmmeter. Obviously, the reached leakage resistances (cf. Table 2) provided sufficient insulation against short-circuits. The type B CFS in variant I had the highest leakage resistance (approximately 990 MΩ).

Integration of the CFS in CF-NCF concrete reinforcement structures

The first approach included the additive structural integration of CFS variant A to the CF rovings running in the 0° or 90° direction of the NCF (Figure 5(a)). The second approach (Figure 5(b)) was concerned with the use of insulated CF rovings of the NCF running in the 0° or 90° directions as sensors. The standard CF warp or weft threads were substituted by the corresponding electrically insulated CFS variant B, according to the requirements of the measurement task. If a spatial resolve measurement of the present tensile loading of the monitored C^3 component is required, two-dimensional or even meandering sensor networks can be implemented by interconnection of the CFS integrated in the warp and weft directions.

The CFS can be inserted into the CF reinforcement structure as a one- or two-dimensional strain sensor

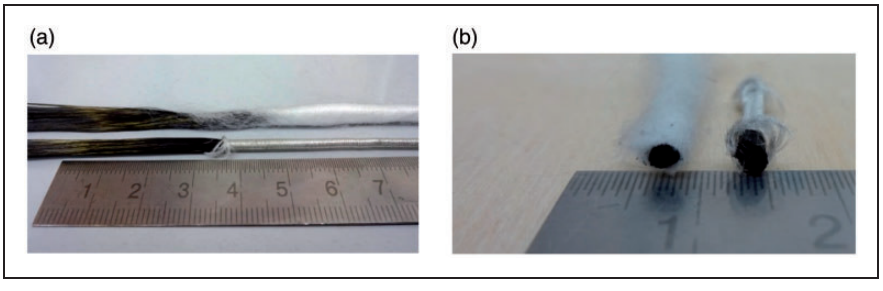

Figure 4. The 50k carbon fiber sensor (CFS) with DREF spun polyester (PES) staple fiber-based (a) and PES filament braided (a) cladding; cross-sectional views (b; left: DREF cladding; right: braided cladding).

Table 2. Specific electrical values of electrically isolated carbon fiber sensors (CFSs)

CFS type		Type A: 1 k CF roving	Type B: 50 k CF roving
Lineic Resistance	DREF I	439.8 ± 4 Ω/m	9.38 ± 0.1 Ω/m
	BRAIDING II	447.2 ± 3 Ω/m	8.7 ± 0.04 Ω/m
Leakage resistance	DREF I	≈365 MΩ	≈990 MΩ
	BRAIDING II	≈620 MΩ	≈410 MΩ

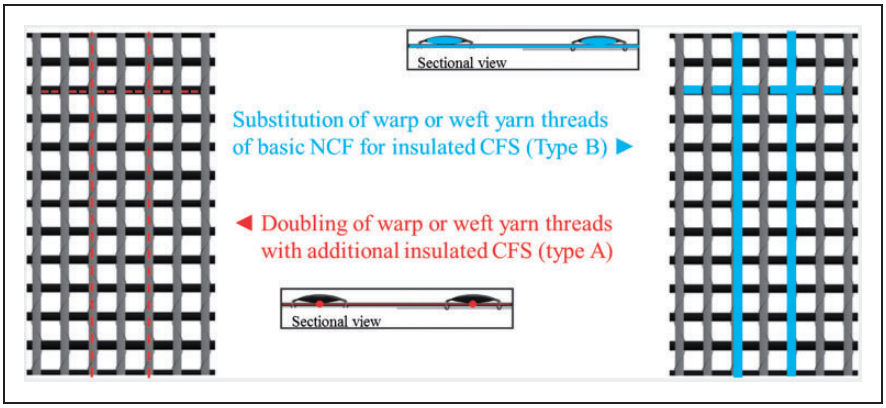

Figure 5. Concepts for one- or two-dimensional sensor integration: additive integration of supplementary carbon fiber (CF) rovings (a) or substitution of defined CF rovings by insulated sensor threads inside of the CF-non-crimp fabric (NCF) (b).
CFS: carbon fiber sensor.

during fabric formation by means of warp-knitting, for example, the multiaxial warp-knitting machine Karl Mayer MALIMO 14024 (Figure 6). By default, they were fixed force-fit against the 90° weft yarns by means of PES binder yarns in a tricot weave with counter-notation arrangement and 4.0 mm stitch spacing, either additively (type A) or substituting (type B) the 50 k standard warp threads of the basic structure.

Two different sensor layouts were examined: a stretched (layout 1, Figure 7(a)) and a meandering (layout 2, Figures 7(b) and (c)) integration of the CFS in the warp direction. In the one-dimensional sensor variant in layout 1, that is, with direct placement of the sensors on the CF warp yarn system running in the 0° direction (Figure 7(a)), the force-fit connection generated by the number of interlacing points with the PES binder yarn was decisive for an excellent, strain-correlated recording capacity of the textile strain sensor. Due to the pre-defined major load distribution direction of the C^3 reinforcement in the warp direction, in which the anisotropically designed CF-NCF exhibited a reinforcement factor of 25.6 in comparison to the 90° (weft direction), the actively measuring areas of the CFS ran in the 0° direction.

To improve the force-fit connection with the load-distributing CF-NCF, the CFS for layout 2 was integrated meanderingly over one warp yarn (Figures 7(b) and (c)) in the projected load transmission areas of the C^3 component on both sides of the 200 mm-long sensitive area of the CFS. The main sensitive part of the CFS is orientated in the major tensile-load or warp direction, respectively.

To improve handling for the later insertion into concrete, to reduce filament damage, improve structural fixation and increase CF/concrete matrix adhesion, the produced NCF was coated with a 15% styrene-butadiene rubber (SBR) dispersion by means of inline padding, and dried before winding in a two-step infrared (IR) heating field at 80–155°C. Depending on the degree of coating, area-related masses of up to 440 g/m^2 were attained. Without further preparation, these products could be processed into C^3 components with fine-grain concrete, using manual lamination or pouring methods. These components could be demolded after 2 days of hydration, and were completely set after 28 days. The tensile force transfer from concrete into load-distributing textile C^3 reinforcement was primarily ensured by a substance-to-substance connection between the concrete matrix and SBR coating on the CF-NCF structure, and secondly by the concrete diffusing through the grid of the biaxial CF-NCF, where it consolidated.

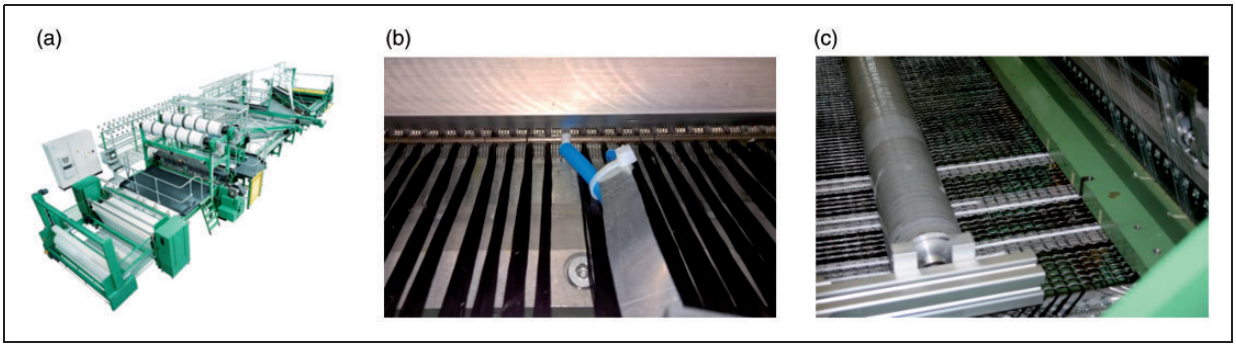

Figure 6. MALIMO 14024 warp-knitting machine (a), bypass feeding of insulated sensor threads in the working area (b) and integration in warp direction of a carbon fiber-non-crimp fabric for C^3 applications (c).

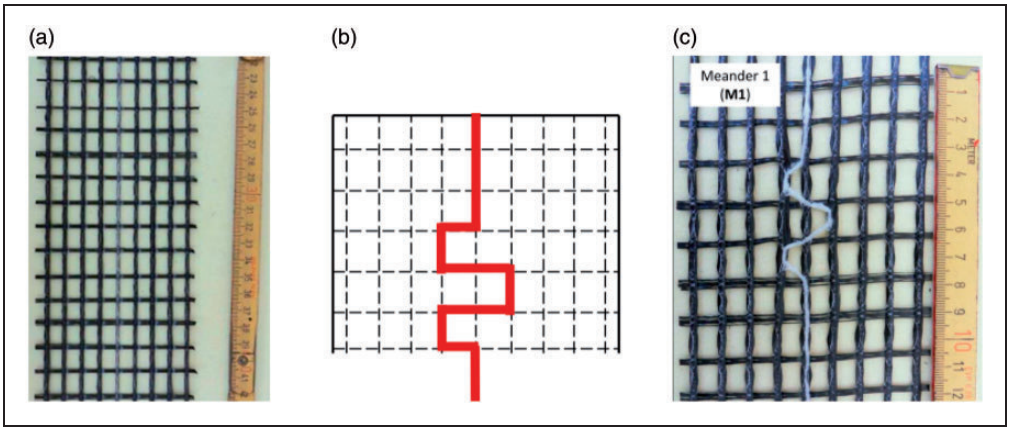

Figure 7. (a) Straight aligned integration of the carbon fiber sensor (CFS) (layout 1) – major load direction of C^3 component is in direction of the folding meter – and (b) meandering integration (layout 2) of the CFS deflected over one warp thread (both-sided) of its sensitive area (c).

Electrical contacting of the CFS

For the electrical interconnection of the sensor threads with measuring electronics (amplifier, multimeter, etc.) outside the projected C^3 component, a practical composite-compatible and corrosion-resistant contacting is required. One effective approach was creating a force-fit connection between the tips of 1 k CFS variants (type A) placed in metallic end splices of 0.1 m^2 due to the small roving cross-section of 0.044 mm^2 using PUR-200-1 W conductive adhesive (Future Carbon GmbH) on the basis of polyurethane mixed with carbon nanotubes (cf. Figure 8(a)). End splices of 2.0 mm^2 were directly crimped onto the tips of the 50 k CFS variants (type B) (cf. Figure 8(b)). Direct crimping without significant filament breakage was conducted successfully only with the type B CFS. Stranded copper wires were soldered onto the metal end splices. These wires served to connect the CFS to measuring electronics outside of the C^3 component.

Manufacturing of C^3 and electro-mechanical characterization

To evaluate the electro-mechanical and sensory recording behavior of one-dimensional sensors made from insulated CF, C^3 specimens with dimensions $L \times W \times H = 400 \times 100 \times 12\,mm^3$ (Figure 9) were produced from three equidistant layers of biaxial CF-NCF. Therefore, the CF-NCF layers were stacked horizontally between 3.0 mm spacers in the sheathing and remained pre-tensioned until the concrete cured. This ensures a homogeneous crack distribution across the tensile-strained specimen area. The observed median crack distance was roughly equal to the weft yarn density of the NCF, that is, 14 mm. The layer arrayed centrally at the level of the neutral fiber carries the CFS; the two symmetrical layers without sensors acted as strength carriers for the concrete reinforcement. After inserting the CF-NCF into an appropriate sheathing (Figure 10(a)), a custom fine-grain concrete mix M690

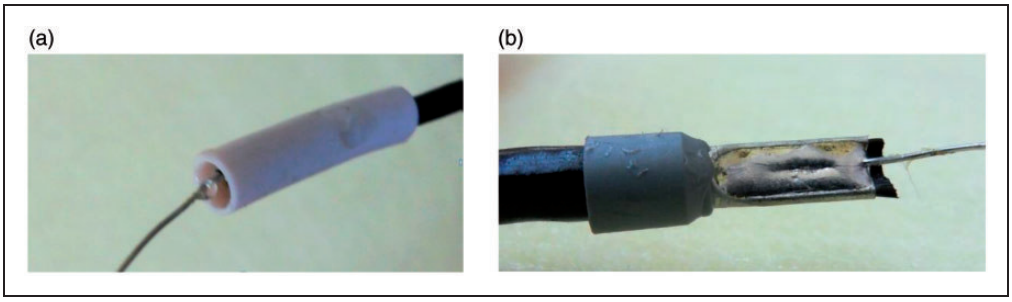

Figure 8. Electrical contacting of type A (a) and type B carbon fiber sensors (b) using conventional cable end sleeves.

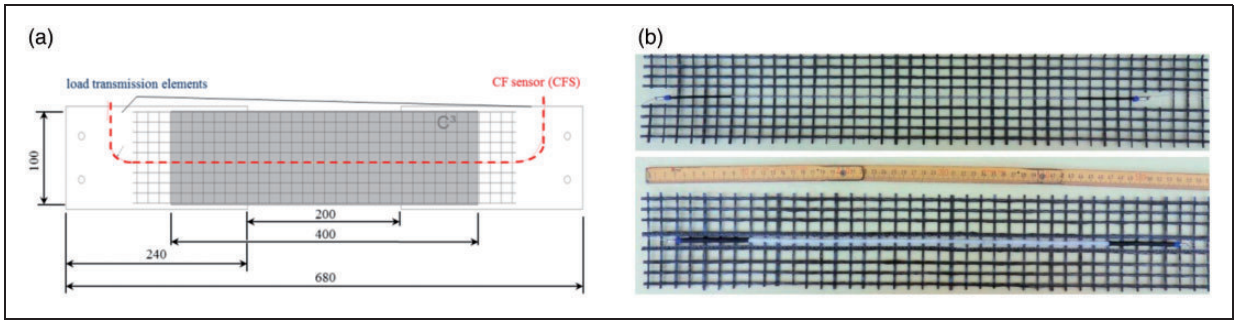

Figure 9. C^3 specimen dimensions of layout 1 in mm (a) and tailored carbon fiber (CF)-non-crimp fabric reinforcement structure ready-to-concrete-cast with electrical contacting on the type A-1 (a) and type B-1 carbon fiber sensor (CFS) ends (b).

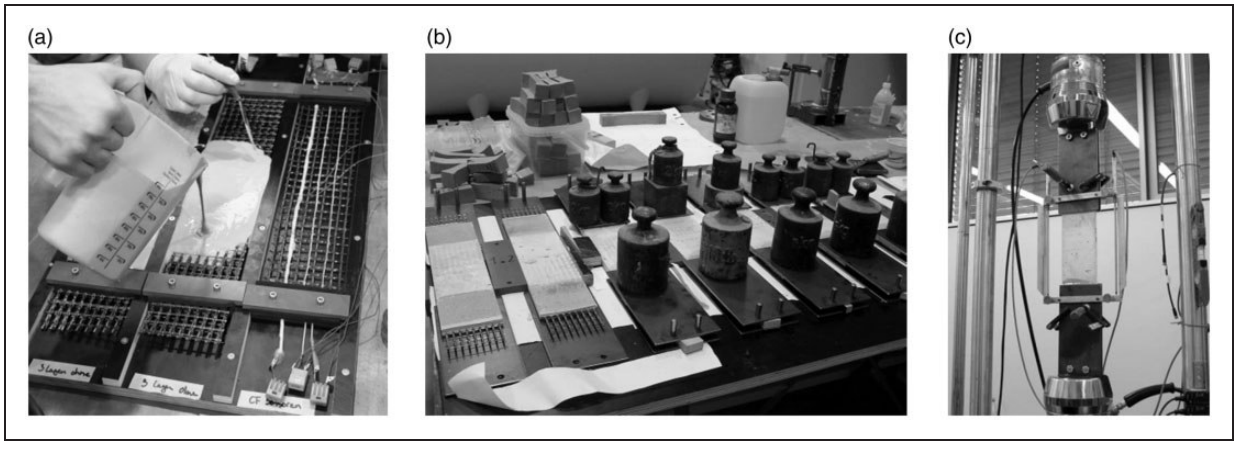

Figure 10. Pouring of C^3 specimens with integrated textile-based sensors (a), (b) and INSTRON 8501 tensile testing machine with clip-on extensometer (c).

(560 g cement C^3 Nanodur CEM III, 142 g rock flour M500, 264 g rock flour M4, 325 g fine sand BCS413, 783 g sand 0/1, 7.12 g flux agent VP 150624-01 and 0.221 water) with 1.0 mm maximum grain size was poured manually without densification, and the casing was removed after 24 hours. The accredited concrete system $PAGEL_{23}$ for the TUDALIT C^3 structures is not used in this studies.

After 6 days of consolidation under climate conditioning of the specimen according to DIN 18555-3, both ends of the specimen were surficial adhesive bonded with two steel plates acting as load transmission elements (cf. Figure 10(b)). The adherend was 100×100 mm^2. These enabled the testing of the specimens on the INSTRON 8501 tensile testing machine (Figure10(c)) without compressive and notch stresses. For evaluating the accuracy of the CFS, the elongation was measured simultaneously with an incremental clip-on extensometer consisting of two inductive standard displacement transducers HBM WSF 50 with 50 mm

nominal displacement. They were orientated parallel to the major tensile-load direction in a clip-on mount. The mount was fixed on the load transmission elements of the specimen whereby its tensile-loaded base length of 200 mm was covered completely.

Results and discussion

Sensor behavior of the CFS in carbon concrete composite C³

The C^3 specimens underwent five load cycles between 2.85‰ and 3.75‰ strains and a final quasi-static load until full structural failure (Figure 11(a)). The change in resistance of the CFS within the concrete that was generated by these strains was measured continuously with the two-probe method using a FLUKE 8846 A laboratory ohmmeter. The measuring data was recorded by means of a DAQ application implemented in the LabVIEW® environment.

The complete failure of the C^3 specimen occurred at 740 ± 50 MPa tensile tension and 7.9 ± 0.8‰ elongation after five previously completed load cycles up to approximately 3.75‰. Figure 11(b) shows a characteristic strain measurement, in which cracks of the concrete matrix can be identified qualitatively up to 12.5 kN and 2.0‰ elongation. Higher tensile loads were carried exclusively by the CF-NCF, which matches the established experiential values[1,2,7,8] of textile-reinforced, tensile-loaded concrete components.

The response characteristics of CFS types A and B in the C^3 component are shown in Figure 12 for both variants with friction-spun (variant I) and braided (variant II) PES cladding material. This identifies a CFS with 50 k CF roving and braided PES cladding (layout 1 CFS, type B, variant II) as the type of strain sensor with the most suitable response characteristics for structural monitoring tasks in C^3 components. These CFSs displayed reproducible specific sensor values with an average gage factor $k = 0.54 \pm 0.02$, an average linearity deviation $A_{Lin} = 5.51 \pm 1.9\%$ and an average hysteresis $A_{Hys} = 2.47 \pm 0.2\%$ over five load cycles. In each case, a good temporal correlation with the tensile straining of the C^3 specimens was apparent (cf. Figure 12).

Table 3 shows the sensor characteristic values for the CFS in layout 1 and highlights that, measured by the gage factor k, CFSs with type A CF roving (1 k 67 tex) in comparison to CFSs with type B CF roving (50 k 3300 tex) displayed a more pronounced change in sensitivity. However, their transmission behavior became unstable with an increasing number of cycles-to-failure. This was probably due to the structural alignment processes of the CFS filaments in the major load direction or an insufficient connection of the CFS to the sensor-carrying reinforcement textile or the surrounding concrete matrix. The indicated negative tensile strain measured by the type A-I CFS resulted from short-circuits with the CF reinforcement structure of the C^3 specimen. Short-circuits occur due to protruding CF filaments from the cladding, which then contact the CF-NCF. Therefore, the stress-related changes in the CFS resistance R were nominally smaller than their base resistance R_0 because of the parallel interconnection with the intrinsically electro-conductive CF reinforcement structure. Previous examinations concerning a CFS made from 1 k CF roving integrated in thermoplastic fiber-reinforced polymer composite (FRPC)[16] discovered a steady decrease in sensitivity with increasing numbers of cycles-to-failure, and a convergence to an asymptotic final value. This distinct behavior was only exhibited by CFS type B in the C^3. CFS type A-II showed the highest k factor within the investigated test series. Generally, CFS type B exhibited only a small change in sensitivity in the sampled range, even after advanced loading and multiple load cycles. Regardless of their gage factor k, their nonlinearity A_{Lin} was, on average, smaller by a factor of 3 than in CFS type A.

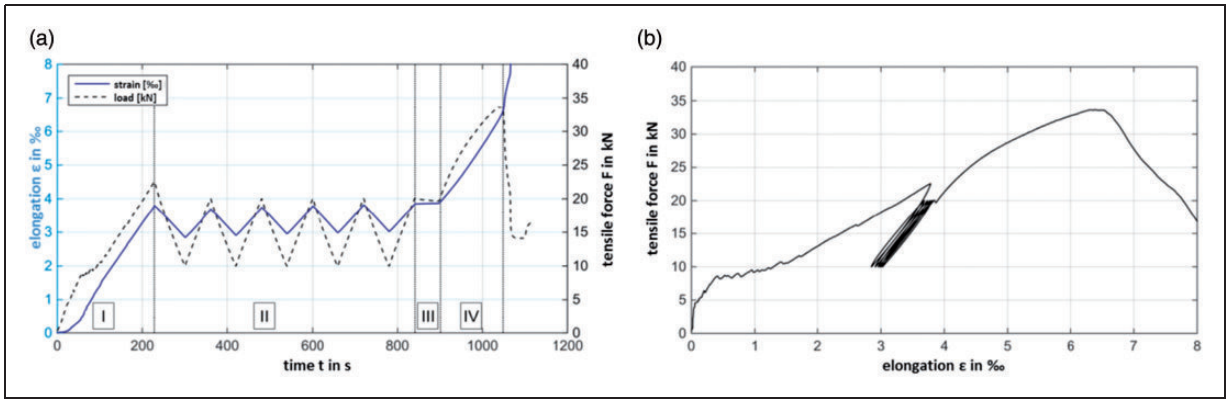

Figure 11. Tensile load profile for determining electro-mechanical behavior of C^3 and of the integrated carbon fiber sensor (a) and force–strain behavior during cyclical loading (b).

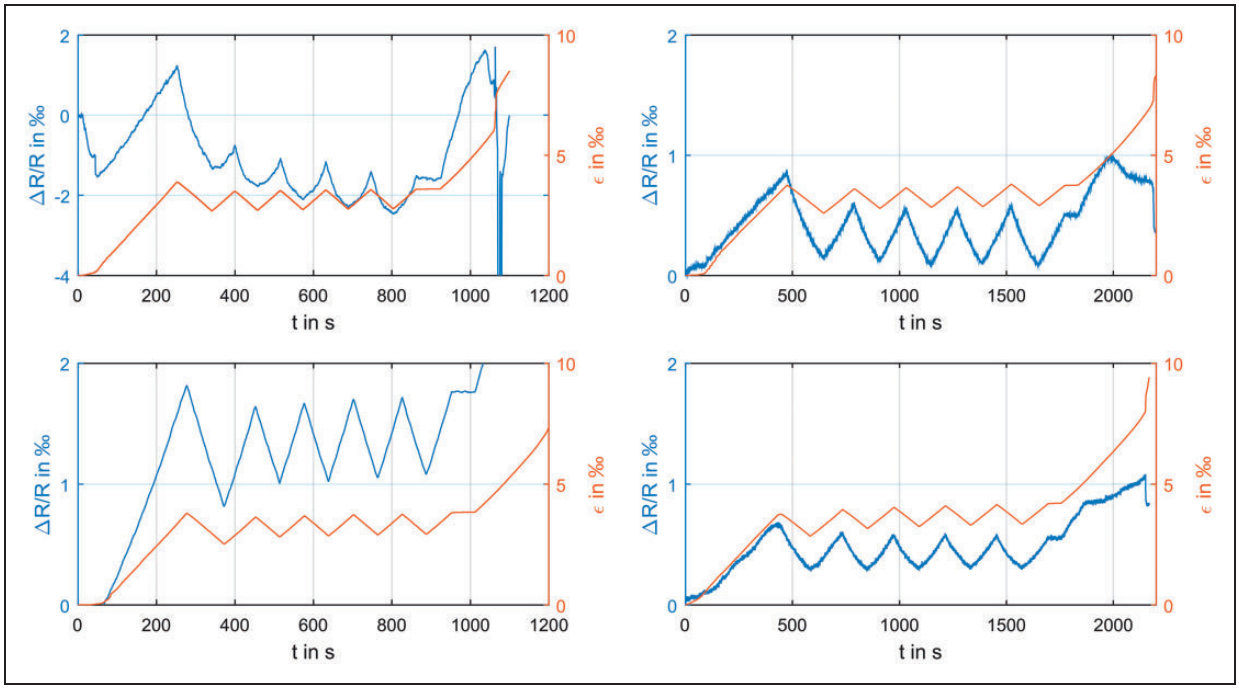

Figure 12. Example response behavior for carbon fiber sensor (CFS) with friction-spun polyester (PES) staple fiber cladding and braided PES multifilament cladding (real tensile strain measured by clip-on extensometer: red graph; indicated tensile strain measured by CFS: blue graph). (Color online only.)

Table 3. Sensor characteristic values of carbon fiber sensors (CFSs) with layout I during cyclical tensile tests

CFS type and variant	1st cycle	2nd cycle	3rd cycle	4th cycle	5th cycle
Gage factor k					
Type A-I	0.61 ± 0.3	0.56 ± 0.3	0.57 ± 0.3	0.56 ± 0.3	0.56 ± 0.3
Type A-II	1.23 ± 0.6	0.88 ± 0.3	1.10 ± 0.3	0.95 ± 0.4	0.27 ± 1.1
Type B-I	0.33 ± 0.1	0.29 ± 0.04	0.32 ± 0.03	0.31 ± 0.05	0.29 ± 0.1
Type B-II	0.57 ± 0.1	0.55 ± 0.03	0.54 ± 0.04	0.52 ± 0.04	0.53 ± 0.1
Nonlinearity A_{Lin} in %					
Type A-I	5.1	5.2	4.1	6.6	5.2
Type A-II	20.1	19.5	13.6	22.4	33.0
Type B-I	11.9	8.5	6.1	6.5	6.4
Type B-II	8.7	5.8	4.9	4.1	4.0
Hysteresis A_{Hys} in %					
Type A-I	3.4	5.2	4.2	3.2	4.1
Type A-II	12.1	18.0	8.0	16.9	19.1
Type B-I	4.2	4.4	4.6	3.2	3.7
Type B-II	2.5	2.7	2.7	2.2	2.3

Type A. . .1 k 67tex CF type B. . .50 k 3300tex CF variant I. . .DREF variant II. . .BRAIDING

The determined hysteresis A_{Hys} caused by cyclic tensile loading was, on average, smaller by a factor of 4 in CFS type B than in CFS type A.

The CFS braided with PES filament yarn (variant II) showed higher gage factors k, regardless of their basic material. This is due to two factors: the pull-off force during braiding or the compression force effect caused by the cross-braided PES filament cladding orthogonal to the CFS longitudinal axis, and the resulting homogeneous alignment of the individual filaments of the CF roving in the projected major load direction of the sensor-carrying C^3 specimen. In friction spinning

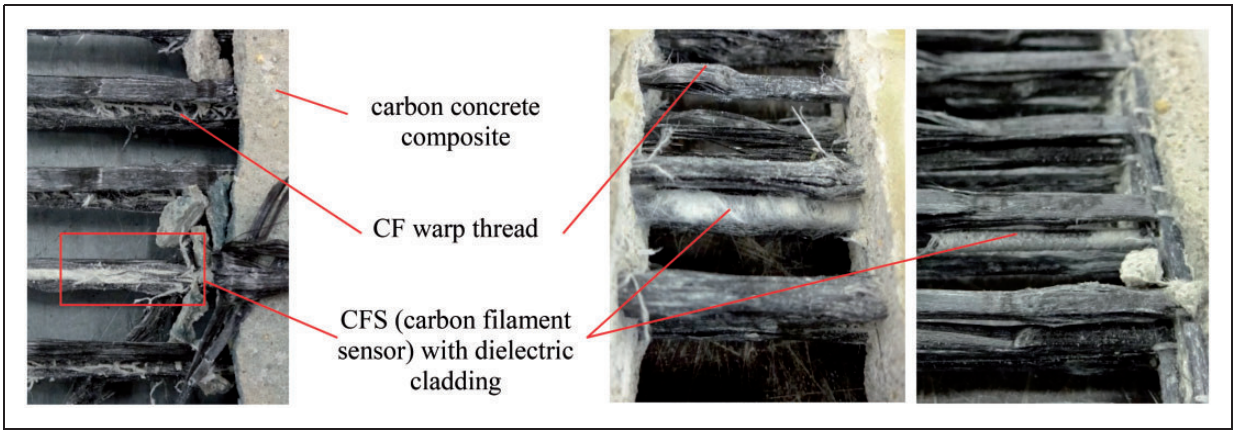

Figure 13. Carbon fiber sensor (CFS) type A-I covered by standard carbon fiber (CF) warp thread (a), standard warp thread substituted by CFS type B-I (b) and type B-II (c) after rupture of the cyclical tensile stressed C^3 specimen.

(variant I), the degree of pre-orientation of the CF filaments in the projected major load direction was lower due to a method-inherent twist insertion of the CF core yarn of 1.0–3.0 m^{-1}. This was found in previous research efforts[24] and leads to a 30% decrease of tensile strength. The inserted twist can cause premature breaking of the outer filaments of the CF roving, which will experience a particular effect under cyclic loads, also referred to as telescopic mode of failure.[25,26] This process is irreversible, so that the ohmic basic resistance of the CFS successively increases, causing a negative drift of the relative change of resistance mapped over the strain, with an increasing number of load changes. This results in the observed decrease of determined sensitivity or gage factor k, respectively.

A visual assessment of the tested C^3 specimens showed furthermore that the type A CFS was completely enclosed by the standard warp thread (Figure 13(a)). Because adhesion between concrete and CF standard warp thread is normally ensured by the SBR coating, the CF sensor thread could not be entirely soaked within the CF standard warp thread in this case. Therefore, small cyclic loads could not be transferred immediately into the CFS, only causing a measurable response at higher loading of the sensor-carrying C^3. CFS type B with both DREF cladding (Figure 13(b)) and braided cladding (Figure 13(c)) was enclosed by the SBR coating and directly covered by the concrete matrix. Due to the larger roving cross-section of approximately 1.8 mm^2 and the larger cladding area enclosed by the concrete matrix along the CFS integration path, a higher interlaminar shear strength of CFS type B than in CFS type A with only 0.04 mm^2 cross-section can be assumed. Also, the SBR coating on CFS type B can act as an immediate adhesive.

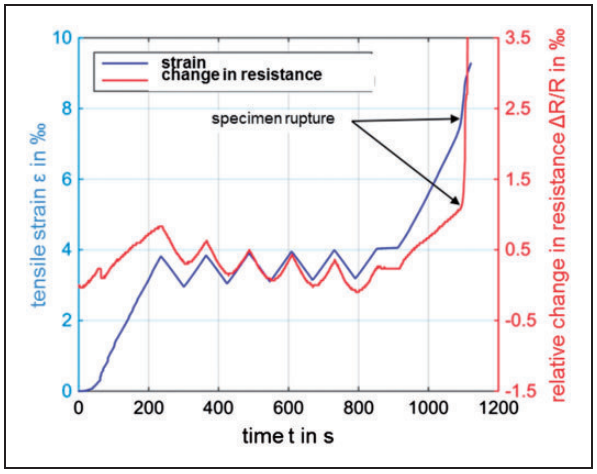

Figure 14. Response characteristics of carbon fiber sensor type A with polyester-DREF cladding in layout 2 with deflection of the sensor thread over a warp thread.

In comparison to the straight aligned CFS (layout 1), the examined layout 2 with the meandering deflected CFS in the load transmission area unexpectedly showed no improvement of its recording behavior on the mechanical strain present in the C^3 specimen (cf. Figure 14). The force insertion into the sensitive part of the CFS layout 2, which is oriented in the major load direction, with lateral deflection of the CFS over a standard warp thread was sufficient, but could not be significantly increased in comparison to sensors with layout 1. The relation between elongation and measurable change in resistance was largely nonlinear, especially with lateral deflection of the CFS from the major load direction over two standard warp threads. Therefore, no sensor parameters of the CFS with layout 2 are given here.

Conclusions

Using tensile tests performed on textile concrete composite (C^3) specimens reinforced with NCF structures from CFs and piezo-resistive CFSs equipped with dielectric fiber cladding, fundamental knowledge regarding sensor and C^3 composite characteristics could be gained, which will contribute greatly to an improved understanding of textile concrete as a building material.

Two types of CFs were examined as textile strain sensors – 67 tex CF roving (type A) and 3300 tex CF roving (type B), each of which were equipped with PES staple fiber cladding (variant I) or PES filament-based (variant II) cladding. Type A CF roving was chosen for the integration into the CF-NCF reinforcement structure. Type B CF roving was chosen for substituting the standard warp yarn system of the CF-NCF reinforcement structure. It can act as both reinforcement and sensor thread.

The preferred sensor solution for application in C^3 components are resistive CFSs from 50 k CF roving with a braided cladding from PES filament (type B-II) in layout 1, that is, straight aligned. They display a gage factor $k = 0.54 \pm 0.02$ at a linearity deviation $A_{Lin} = 5.51 \pm 1.9\%$ in a measured range of up to 3.75‰ tensile strain. The observed decrease in sensitivity (gage factor k) is presumably caused by structural setting and alignment processes of the CFS filaments under cyclic loading of the C^3. Furthermore, an insufficiently strong force-fit connection of the CFS to the load-distributing biaxial NCF structure or the concrete matrix is mainly responsible for the determined response characteristics of the textile sensors. However, this could not be proven in this article. The presented fiber-based piezo-resistive in situ sensors allow conclusions regarding the interior structure, integrity or mechanical/thermal load state of C^3 components, offering a potential measuring possibility for Smart Home applications or the decentralized remote diagnosis of larger buildings or building complexes, for example, facades of multifunctional C^3 building envelopes or C^3 supporting structures. Compared to conventional sensor solutions, the approach of similar sensor materials and the integrated production of CFSs in the textile-technological production of CF-based reinforcement structures offers great advantages, including composite compatibility, time savings during production, measuring point protection and scalability of the CFS.

Declaration of conflicting interests

The authors declared no potential conflicts of interest with respect to the research, authorship and/or publication of this article.

Funding

The authors disclosed receipt of the following financial support for the research, authorship, and/or publication of this article: The collaborative research project 03ZZ0305P "*Carbon Concrete Composite C^3 – Basic Project B4 – Multifunctional Components from C^3 – Subproject C^3Sense | Integration of Sensors*" of the Projekttraeger Juelich (PTJ) was supported from funds of the Federal Ministry of Education (BMBF). The IGF research project 18901BR/1 of the research association "Forschungskuratorium Textil (FKT) e. V." is funded through the AiF within the program for supporting the industrial collective research ("Industrielle Gemeinschaftsforschung", IGF) from funds of the Federal Ministry of Economics and Energy (BMWi) by a resolution of the German Bundestag.

References

1. Special research field SFB 528 - Textile reinforcement for the structurally engineered strengthening and maintenance - Finale report. Technische Universitaet Dresden, 08.05.2012, http://nbn-resolving.de/urn:nbn:de:bsz:14-qucosa-86425 (accessed 30 August 2016).
2. Curbach M (ed.) and Ortlepp and R (ed.) Textile reinforced concrete in theory and practice. In: *proceedings of the 6th colloquium of textile reinforced structures (CTRS6) - concluding colloquium of the special research fields SFB 528 (Dresden) and SFB 532 (Aachen)*, Berlin, 19–20 September 2011. p.444. Dresden, Technisch Universitaet Dresden. ISBN 978-3-86780-245-1.
3. Method for the strengthening of ferroconcrete by TUDALIT (textile reinforced concrete). Deutsches Institut für Bautechnik (DIBt): General technical approval, http://www.textilbetonzentrum.de/app/download/5806918971/AbZ_Z-31.10-182.pdf (accessed 28 August 2017).
4. Haque ME, Zain MFM, et al. Recent application of structural civil health monitoring using WSN and FBG. *World Appl Sci J* 2012; 20: 585–590.
5. Li H-N, Li D-S and Song G-B. Recent applications of fiber optic sensors to health monitoring in civil engineering. *Eng Struct* 2004; 26: 1647–1657.
6. Chang PC, Flatau A and Liu SC. Review paper: health monitoring of civil infrastructure. *Struct Health Monitor* 2003; 2: 257–267.
7. Goldfeld Y, Rabinovitch O, Fishbain B, et al. Sensory carbon fiber based textile-reinforced concrete for smart structures. *J Intell Mater Syst Struct* 2016; 27: 469–489.
8. Goldfeld Y, Ben-Aarosh S, Rabinovitch O, et al. Integrated self-monitoring of carbon based textile reinforced concrete beams under repeated loading in the un-cracked region. *Carbon* 2015; 98: 1–38.
9. Wen S and Chung DDL. Electrical-resistance-based damage self-sensing in carbon fiber reinforced cement. *Carbon* 2007; 45: 710–716.
10. Wen S and Chung DDL. Self-sensing of flexural damage and strain in carbon fiber reinforced cement and effect of

embedded steel reinforcing bars. *Carbon* 2006; 44: 1496–1502.
11. Wen S, Wang S and Chung DDL. Piezoresistivity in continuous carbon fiber polymer-matrix and cement-matrix composites. *J Mater Sci* 2000; 35: 3669–3675.
12. Teomete E. Measurement of crack length sensitivity and strain gage factor of carbon fiber reinforced cement matrix composites. *Measurement* 2015; 74: 21–30.
13. Yang CQ and Wu ZS. Self-structural health monitoring function of RC Structures with HCFRP sensors. *J Intell Mater Syst Struct* 2006; 17: 895–906.
14. Heinrich M, Kroll L, Gelbrich S, et al. manufacturing of strain gages for the integral monitoring of civil engineering construction works in concrete structures by using etching embroidery method. In: Jacquline T (ed.) *proceedings of the 15th Chemnitzer Textiltechnik Tagung*, Chemnitz, 31 May–1 June 2016, pp.52–56.
15. Owston CN. Electrical properties of single carbon fibres. *J Phys D Appl Phys* 1970; 3: 1615–1626.
16. Haentzsche E, Matthes A, Nocke A, et al. Characteristics of carbon fiber based strain sensors for structural-health monitoring of textile-reinforced thermoplastic composites depending on the textile technological integration process. *Sens Actuat A Phys* 2013; A203: 189–203.
17. Haentzsche E, Unger R, Nocke A, et al. Carbon filament yarn-based sensor networks for spatially resolved monitoring of fiber-reinforced composites. *Tech Text* 2014; 57: 22–25.
18. Cherif Ch, Haentzsche E, Mueller R, et al. Carbon fibre sensors embedded in glass fibre-based composites for wind turbine blades. In: *Smart textiles and their applications*. Cambridge, MA: Woodhead Publishing Series in Textiles: Number 178. Woodhead Publishing, 2016, pp.329–352.
19. Haentzsche E, Mueller R, Huebner M, et al. Manufacturing technology of integrated textile-based sensor networks for in situ monitoring applications of composite wind turbine blades. *J Smart Mater Struct* 2016; 25: 105012.
20. Bridgman P W. The Effect of Tension on the Electrical Resistance of Certain Abnormal Metals. Proceedings of the American Academy of Arts and Sciences 57(1922)3, pp.41-66, DOI: 10.2307/20025885
21. Wen S and Chung DDL. Piezoresistivity in continuous carbon fiber cement-matrix composite. *Cem Conr Res* 1999; 29: 445–449.
22. Fehrer E, Fuchs H and Konig F. *Apparatus for spinning textile fibers*. Patent US4107909, USA, 1977.
23. PAGEL/TUDALIT Fine Concrete TF10. Product datasheet. PAGEL SPEZIAL-BETON GMBH & Co. KG, http://www.pagel.com/all/pdf/gb/tf10_gb.pdf (accessed 30 August 2016).
24. Hasan MMB, Diestel O and Cherif Ch. Electro-mechanical properties of friction spun conductive hybrid yarns made of carbon filaments for composites. *Text Res J* 2011; 81: 1603–1616.
25. Banholzer B, Brockmann T and Brameshuber W. Material and bonding characteristics for dimensioning and modelling of textile reinforced concrete (TRC) elements. *Mater Struct* 2006; 39: 749–763.
26. Weber WE and Mechtcherine V. Modeling the dynamic properties of fibre-reinforced concrete with different coating technologies of multifilament yarns. *Cem Concrete Compos* 2016; 73: 257–266.